Articles

Coordination Complexes Derived from Tri-, Tetra-, and Pentaphosphoxane Rings

Edward H. Wong,* Xiaoyong Sun, Eric J. Gabe, Florence L. Lee, and Jean-Pierre Charland

Department of Chemistry, University of New Hampshire, Durham, New Hampshire 03824, and Chemistry Division, National Research Council of Canada, Ottawa, Canada K1A 0R9

Received March 18, 1991

Thermal reactions of hexacarbonylchromium and -tungsten with bis(diisopropylamino)phosphine oxide yielded the tetraphosphoxane complexes *cis*-$M(CO)_4[^iPr_2NPO]_4$ as the major products. Spectral data and X-ray structural determination of the molybdenum analogue confirmed 1,5-coordination of statistical mixtures of the chair–boat (C_s) and chair–chair (C_{2v}) conformations of the P_4O_4 ring. Crystal data: monoclinic, $A2/a$; $a = 18.992$ (1), $b = 11.306$ (5), $c = 19.368$ (1) Å; $\beta = 98.63$ (1)°; $V = 4111.6$ (4) Å^3; $Z = 4$; final $R_F = 0.062$, $R_{wF} = 0.057$ for 2219 significant reflections and varying 204 parameters. Minor coproducts from the chromium reaction included $Cr_2(CO)_8[^iPr_2NPO]_4$, with a tetradentate P_4O_4 ring chelating both metals, as well as $Cr_2(CO)_7[^iPr_2NPO]_5$. The latter structure features a novel pentaphosphoxane P_5O_5 ring coordinated to one $Cr(CO)_3$ and one $Cr(CO)_4$ to form a bimetallic cage. Crystal data: monoclinic, $P2_1/c$; $a = 12.6554$ (8), $b = 17.639$ (1), $c = 23.670$ (1) Å; $\beta = 101.82$ (1)°; $V = 5171.7$ (5) Å^3; $Z = 4$; final $R_F = 0.088$, $R_{wF} = 0.081$ for 4337 significant reflections and varying 491 parameters. Under milder reaction conditions with molybdenum hexacarbonyl, a triphosphoxane complex $Mo(CO)_5[^iPr_2NPO]_3$ can be isolated. Crystal data: orthorhombic, $Pbc2_1$; $a = 11.570$ (2), $b = 18.729$ (5), $c = 32.056$ (3) Å; $V = 6946.36$ Å^3; $Z = 8$; final $R_F = 0.047$, $R_{wF} = 0.048$ for 3469 significant reflections and varying 685 parameters. This was converted readily by heating to the known $Mo_2(CO)_8[^iPr_2NPO]_4$ cage complex. Reactions of the parent $[^iPr_2NPO]_3$ triphosphoxane ring with $Mo(CO)_4$(norbornadiene) afforded a 1:1 complex *cis*-$Mo(CO)_4[^iPr_2NPO]_3$ which also transformed into the same adamantanoid cage complex upon warming. With bis(benzonitrile)palladium dichloride, triphosphoxane gave a product characterized by spectral data and X-ray crystallography to be *cis*-$PdCl_2[^iPr_2NPO]_4$ with a 1,5-coordinated tetraphosphoxane ring exclusively in the chair–chair (C_{2v}) conformation. Crystal data: monoclinic $C2/c$; $a = 19.980$ (5), $b = 11.0945$ (10), $c = 17.934$ (9) Å; $\beta = 112.04$ (3)°; $V = 3684.8$ Å^3; $Z = 4$; final $R_w = 0.051$ and $R_{wF} = 0.060$ for 252 variables using 3246 significant reflections. A similar reaction with $NiBr_2{\cdot}DME$ (DME = dimethoxyethane) yielded instead a 1,3-coordinated P_4O_4 complex $NiBr_2[^iPr_2NPO]_4$. The parent $[^iPr_2NPO]_4$ ligand, stable below −20 °C, can be liberated from this Ni complex by pyridine substitution. It reverts to the triphosphoxane compound upon warming to ambient temperature.

Introduction

Trivalent phosphorus–oxygen heterocycles or cyclophosphoxanes are rare compared to cyclophosphazanes,[1] cyclophosphazenes,[2] and cyclophosphates.[3] In fact, only three well-characterized P(III)–O rings are known, $[^iPr_2NPO]_3$,[4] $[BHT\text{-}PO]_2$, and $[BHT\text{-}PO]_3$ (BHT = 2,6-di-*tert*-butyl-4-methylphenoxy).[5] Earlier Russian workers reported the synthesis of similar heterocycles by the hydrolysis of dichloroorganophosphines, though the products were only characterized by molecular weight determinations.[6] These species can all be regarded as cyclic head-to-tail oligomers of the unknown phosphinidene oxide $R{-}P{=}O$ monomer.[7] No higher congeners such as the tetraphosphoxane $[RPO]_4$ and pentaphosphoxane $[RPO]_5$ have been previously described. These oligomeric ligands have oxygen-bridged trivalent phosphorous donor sites that can potentially coordinate one or more metals and form rigid polycyclic and cage complexes (Figure 1). Little is known about their coordination modes and steric or electronic ligand influence on metal centers and, conversely, the effect of metal binding on their oligomeric equilibria and ring conformations. Furthermore, it may be reasoned that metal coordination can yield novel polycyclic structures containing phosphoxane heterocycles unknown in the uncomplexed state.

Previously, we have reported the serendipitous assemblage of a bimetallic cage complex of tetraphosphoxane

---

* Address correspondence to this author at the University of New Hampshire.

(1) Zeiss, W.; Schwartz, W.; Hess, H. *Angew. Chem., Int. Ed. Engl.* **1977**, *16*, 407. Gallicano, K. D.; Rettig, S. J.; Trotter, J. *Can. J. Chem.* **1982**, *60*, 2415–2419; **1984**, *62*, 1869–1873. Malavaud, C.; N'Gando M'-Pondo, T.; Lopez, L.; Barrans, J.; Legros, J.-P. *Can. J. Chem.* **1984**, *62*, 43–50. Zeiss, W.; Henjes, H. *Chem. Ber.* **1978**, *111*, 1655–1658. Barendt, J. M.; Bent, E. G.; Haltiwanger, R. C.; Norman, A. D. *J. Am. Chem. Soc.* **1980**, *111*, 6883–6884.

(2) Allcock, H. R. *Chem. Eng. News* **1985**, *63* (11), 22. Allcock, H. R. *Chem. Rev.* **1972**, *72*, 315–356. Allcock, H. R. *Phosphorus-Nitrogen Compounds*; Academic Press, Inc.: New York, 1972.

(3) Baer, E.; Sarma, G. R. *Can. J. Biochem.* **1967**, *45*, 1755–1761. Cherepinskii-Malov, V. D.; Gusev, A. I.; Nuretdinov, I. A.; Struchkov, Yu T. *Zh. Strukt. Khim.* **1971**, *12*, 126–132; *Chem. Abstr.* **1971**, *75*, 11690z. Glonek, T.; Van Wazer, J. R.; Kleps, R. A.; Meyers, T. C. *Inorg. Chem.* **1974**, *13*, 2337–2345. Ogata, N.; Sanui, K.; Harada, M. *J. Polym. Sci., Polym. Chem. Educ.* **1979**, *17*, 2401–2411. Durif, A. *The Chemistry of Inorganic Homo- and Heterocycles*; Haiduc, I., Sowerby, D. B., Eds.; Academic Press: New York, 1987; Vol. 2, Chapter 22.

(4) Niecke, E.; Zorn, H.; Krebs, B.; Henkel, G. *Angew. Chem., Int. Ed. Engl.* **1980**, *19*, 709–710.

(5) Chasar, D. W.; Fackler, J. P.; Mazany, A. M.; Komoroski, R. A.; Kroenke, W. J. *J. Am. Chem. Soc.* **1986**, *108*, 5956–5962. Chasar, D. W.; Fackler, J. P.; Komoroski, R. A.; Kroenke, W. J.; Mazany, A. M. *J. Am. Chem. Soc.* **1987**, *109*, 5690–5693.

(6) Nifant'ev, E. E.; Koroteev, M. P.; Ivanov, N. L.; Gudkova, I. P.; Predvoditelev, D. A. *Dokl. Chem.* (*Engl. Transl.*) **1967**, *173*, 398–401.

(7) Niecke, E.; Englemann, M.; Zorn, H.; Krebs, B.; Henkel, G. *Angew. Chem., Int. Ed. Engl.* **1980**, *19*, 710–712.

0276-7333/91/2310-3010$02.50/0

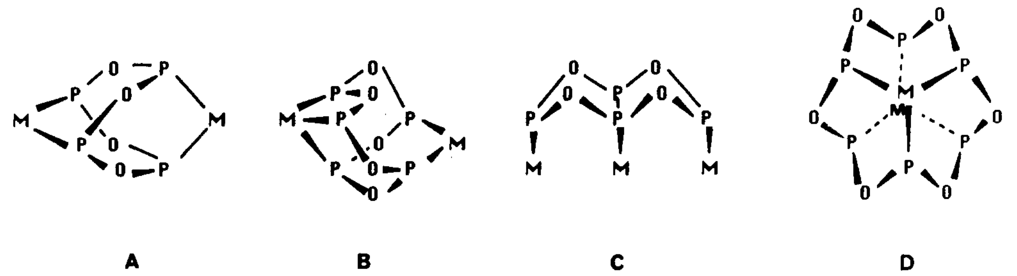

Figure 1.

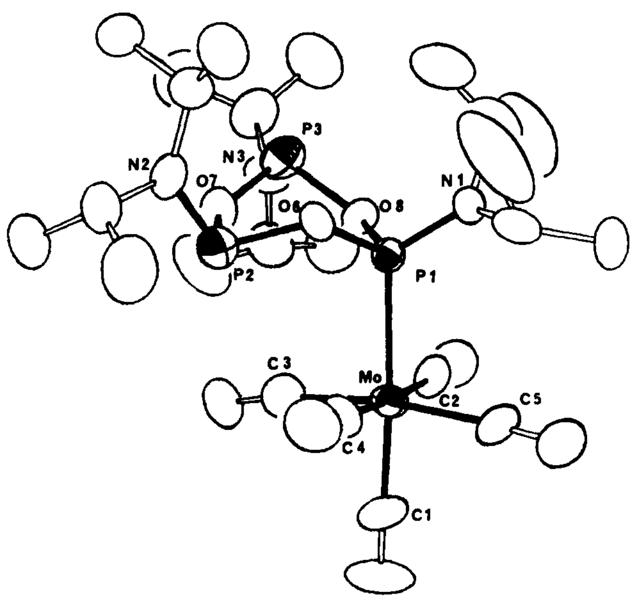

Figure 2. Molecular structure of $\mathrm{Mo(CO)_5[{}^iPr_2NPO]_3}$ (1).

Table I. ^{31}P NMR Data for the Polyphosphoxane Complexes

compd	splitting pattern (δ, ppm) (J, Hz)[a]
$\mathrm{Mo(CO)_5[{}^iPr_2NPO]_3}$ (1)	AMX ($\delta_A = 146.7$, $\delta_M = 139.2$, $\delta_X = 134.1$) ($J_{AM} = 10$, $J_{AX} = 13$, $J_{MX} = 11$ Hz)
$\mathrm{Cr(CO)_4[{}^iPr_2NPO]_4}$ (**3a**)	A_2XY ($\delta_A = 177.4$, $\delta_X = 129.5$, $\delta_Y = 126.8$) ($J_{AX} = 38$, $J_{AY} = 11$, $J_{XY} = 2$ Hz)
3b	A_2X_2 ($\delta_A = 173.4$, $\delta_X = 143.4$) ($J_{AX} = 28$ Hz)
$\mathrm{Cr_2(CO)_8[{}^iPr_2NPO]_4}$ (4)	$\delta = 159.4$
$\mathrm{Cr_2(CO)_7[{}^iPr_2NPO]_5}$ (5)	A_2MX_2 ($\delta_A = 176.6$, $\delta_M = 175.1$, $\delta_X = 156.9$) ($J_{AM} = 9$, $J_{AX} = 0$, $J_{MX} = 40$ Hz)
$\mathrm{W(CO)_4[{}^iPr_2NPO]_4}$ (**6a**)	AB_2X ($\delta_A = 134.0$, $\delta_B = 133.0$, $\delta_X = 128.70$) ($J_{AB} = 49.6$, $J_{AX} = 3.5$, $J_{BX} = 8.8$, $J_{WP(B)} = 166$ Hz)
6b	A_2X_2 ($\delta_A = 147.55$, $\delta_X = 126.16$) ($J_{AX} = 35$ Hz, $J_{WP} = 166$ Hz)
$\mathrm{Mo(CO)_4[{}^iPr_2NPO]_3}$ (7)	A_2X ($\delta_A = 138.5$, $\delta_X = 130.1$) ($J_{AX} = 2$ Hz)
$\mathrm{Mo(CO)_4[{}^iPr_2NPO]_4}$ (**8a**)	A_2XY ($\delta_A = 154.1$, $\delta_X = 128.7$, $\delta_Y = 127.1$) ($J_{AX} = 59$, $J_{AY} = 11$, $J_{XY} = 2$ Hz)
8b	$AA'XX'$ ($\delta_A = \delta_{A'} = 149.8$, $\delta_X = \delta_{X'} = 143.5$) ($J_{AX} = J_{AX'} = 105$; $J_{AA'} = 50$, $J_{XX'} = 5$ Hz)
$\mathrm{PdCl_2[{}^iPr_2NPO]_4}$ (9)	A_2X_2 ($\delta_A = 147.8$, $\delta_X = 88.3$) ($J_{AX} = 44$ Hz)
$\mathrm{NiBr_2[{}^iPr_2NPO]_4}$ (10)	$AA'XX'$ ($\delta_A = \delta_{A'} = 144.4$; $\delta_A = \delta_{A'} = 63.4$) ($J_{AA'} = J_{XX'} = 50$, $J_{AX} = J_{A'X'} = 20$, $J_{AX'} = J_{A'X} = 1$ Hz)
$\mathrm{NiCl_2[{}^iPr_2NPO]_4}$ (11)	$AA'XX'$ ($\delta_A = \delta_{A'} = 144.2$; $\delta_X = \delta_{X'} = 55.7$) ($J_{AA'} = J_{XX'} = 50$, $J_{AX} = J_{A'X'} = 20$, $J_{AX'} = J_{A'X} = 1$ Hz)
$\mathrm{[{}^iPr_2NPO]_4}$	$\delta = 130.7$[b]
$\mathrm{Cr(CO)_4[{}^iPr_2NPO]_4S}$ (12)	A_2MX ($\delta_A = 181.0$, $\delta_M = 135.4$, $\delta_X = 40.2$) ($J_{AM} = 61$, $J_{AX} = 34$ Hz)
$\mathrm{Cr(CO)_4[{}^iPr_2NPO]_4S_2}$ (13)	A_2XY ($\delta_A = 185.5$, $\delta_X = 51.7$, $\delta_Y = 37.2$) ($J_{AX} = 68$, $J_{AY} = 29$ Hz)

[a] All spectra were run in $\mathrm{CDCl_3}$. [b] At −30 °C.

$\mathrm{P_4O_4}$ (type A in Figure 1) from $\mathrm{Mo(CO)_6}$ and $\mathrm{({}^iPr_2N)_2P(O)H}$ (eq 1).[8] We now describe the syntheses of several

$$\mathrm{2Mo(CO)_6 + 4({}^iPr_2N)_2P(O)H \rightarrow Mo_2(CO)_8[{}^iPr_2NPO]_4 + 4CO + 4{}^iPr_2NH} \quad (1)$$

tri-, tetra-, and pentaphosphoxane complexes using $\mathrm{({}^iPr_2N)_2P(O)H}$ as well as the $\mathrm{[{}^iPr_2NPO]_3}$ heterocycle as precursors. Preliminary reports on the syntheses and structures of $\mathrm{Mo(CO)_5[{}^iPr_2NPO]_3}$, *cis*-$\mathrm{Mo(CO)_4[{}^iPr_2NPO]_4}$, and $\mathrm{Cr_2(CO)_7[{}^iPr_2NPO]_5}$ have appeared.[9,10]

Results

Thermal Reaction of $\mathrm{({}^iPr_2N)_2P(O)H}$ with Metal Carbonyls. All group VI metal hexacarbonyls reacted with the phosphine oxide in hot toluene to give products containing either the trimer, tetramer, or pentamer of the phosphinidene oxide $\mathrm{{}^iPr_2N{-}P{=}O}$ as ligands. The ease of CO replacement from $\mathrm{Mo(CO)_6}$ allowed milder reaction conditions (100 °C, 4–6 h) and chromatographic isolation of an intermediate $\mathrm{Mo(CO)_5[{}^iPr_2NPO]_3}$, white complex 1, in 2–5% yield. The molecular structure of this has been determined and is shown in Figure 2. It contains the $\mathrm{[{}^iPr_2NPO]_3}$ ring in a boat form with $\mathrm{Mo(CO)_5}$ coordinated in an axial position. The thermodynamic product, previously identified as the $\mathrm{Mo_2(CO)_8[{}^iPr_2NPO]_4}$ cage complex **2**, readily formed in high yields when 1 was further refluxed in toluene. It was the sole product (80–90% yield) when the reaction was carried out in refluxing toluene for over 6 h (eq 2).

$$\mathrm{Mo(CO)_6 + 3({}^iPr_2N)_2P(O)H \rightarrow \underset{1}{Mo(CO)_5[{}^iPr_2NPO]_3} + CO + 3{}^iPr_2NH}$$

$$\mathrm{2\underset{1}{Mo(CO)_5[{}^iPr_2NPO]_3} \rightarrow \underset{2}{Mo_2(CO)_8[{}^iPr_2NPO]_4} + 2CO + 2[{}^iPr_2NPO]} \quad (2)$$

For $\mathrm{Cr(CO)_6}$ the major product after prolonged reflux (48 h) was a monometallic tetraphosphoxane complex, $\mathrm{Cr(CO)_4[{}^iPr_2NPO]_4}$, isolated as a white solid in 30% yield and containing a 1:2 statistical mixture of the chair–chair (C_{2v}, complex **3a**) and chair–boat (C_s, complex **3b**) conformations. These structural assignments were confirmed by ^{31}P NMR data (Table I) as well as the X-ray structural determination of the molybdenum analogues (**8a**, **8b**) presented below. Minor products included the light yellow chromium complex $\mathrm{Cr_2(CO)_8[{}^iPr_2NPO]_4}$ (4; 48 h reflux, 2% isolated yield), as well as the novel yellow pentaphosphoxane complex $\mathrm{Cr_2(CO)_7[{}^iPr_2NPO]_5}$ (5; over 60 h reflux, 5% yield), both of which can be separated from **3a** and **3b** by recrystallization from hexane. The molecular structure of 5 has been determined and is shown in Figure 3. The $\mathrm{P_5O_5}$ heterocycle is simultaneously coordinated

---

(8) Wong, E. H.; Turnbull, M. M.; Gabe, E. J.; Lee, F. L.; Le Page, Y. *J. Chem. Soc., Chem. Commun.* **1983**, 776–777.

(9) Wong, E. H.; Gabe, E. J.; Charland, J.-P. *J. Chem. Soc., Chem. Commun.* **1988**, 1632–1633.

(10) Wong, E. H.; Gabe, E. J.; Lee, F. L. *J. Chem. Soc., Chem. Commun.* **1989**, 1236–1237.

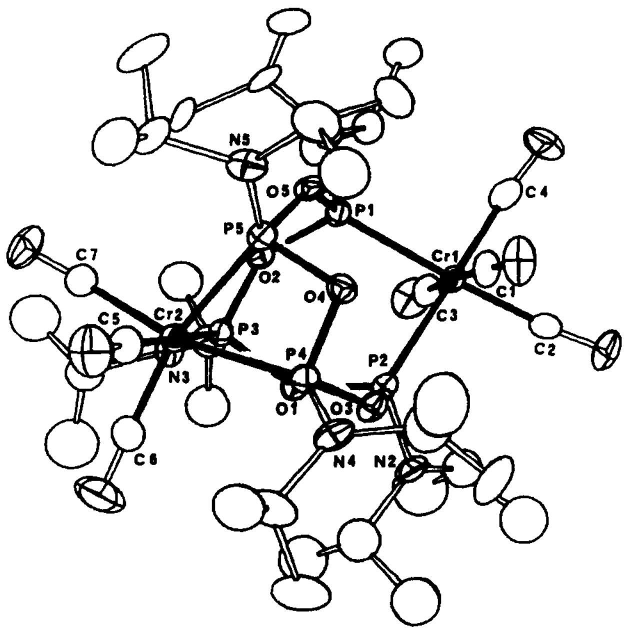

Figure 3. Molecular structure of $Cr_2(CO)_7[{}^iPr_2NPO]_5$ (**5**).

Table II. ^{13}C NMR Data for the Polyphosphoxane Complexes

compd	assgnt (δ, ppm; J, Hz)[a]
1	CO (210.6 doublet (db), J = 39; 205.7 db of db, J = 4, 13); CH (47.3, 46.7, 45.1, 44.5, 44.0, J = 3–4); CH$_3$ (24.5, 24.1, 23.2)
3	CO (224.7, 224.8 triplets, J = 10; 218.0, 217.8 multiplets); CH (46.6, 46.1 triplets, J = 4; 43.3, 43.1, 42.9); CH$_3$ (23.1, 22.0)
4	CO (226.4 triplet, J = 5; 220.0, multiplet); CH (48.4); CH$_3$ (24.4, 23.0)
5	CO (229.6, 228.5, 224.4, 219.6, 216.7); CH (49.0, doublet, 48.5, 47.7, 47.6); CH$_3$ (25.4, 24.8, 24.5, 24.3, 23.7)
6	CO (206.4, 206.1 triplets, J = 12; 202.2, 201.5); CH (48.0, 47.6 triplets, J = 5; 44.8, 44.7, 44.5, 44.2, 44.0); CH$_3$ (24.1, 23.1, 23.0)
7	CO (not avail); CH (47.8 triplet, J = 6; 44.7, 44.4); CH$_3$ (24.4, 23.6, 23.2)
8	CO (214.8, 208.3, 207.2 multiplets); CH (47.3, 46.7, 46.4, 46.1 triplets); CH$_3$ (23.4, 23.1, 22.2)
9	CH (47.7, 47.2); CH$_3$ (23.2, 19.2)
10	CH (48.6, 45.1); CH$_3$ (24.5, 22.9)

[a] All spectra were run in CDCl$_3$ with chemical shifts referenced to the internal TMS standard.

Table III. Proton NMR Data (δ, ppm) for the Polyphosphoxane Complexes

compd	methine region[a]	methyl region[a]
1	3.96 (septet, 6.9 Hz), 3.76 (multiplets)	1.27, 1.26, 1.22, 1.18, 1.15, 1.14 (dbs, 6.9 Hz)
3	3.84 (septet, 6.6 Hz), 3.6 (broad)	1.24 (db, 6.6 Hz), 1.13 (db, 6.1 Hz)
4	4.12 (bd)	1.38 (d, 6.6 Hz), 1.32 (d, 6.7 Hz)
5	4.66 (m), 4.25 (m), 4.17 (m)	1.40 (d, 6.7 Hz), 1.35 (d, 6.1 Hz)
6	3.93 (septet, 6.9 Hz), 3.8 (broad)	1.30 (db, 6.9 Hz), 1.21 (db, 7.1 Hz)
7	3.86 (septet, 6.9 Hz), 3.7 (broad)	1.32, 1.31, 1.26 (dbs, 6.9 Hz)
8	3.95 (septet, 6.8 Hz), 3.8 (broad)	1.29 (db, 6.8 Hz), 1.20 (db, 6.8 Hz)
9	3.74 (multiplets)	1.36, 1.28 (db, 6.7 Hz)
10	4.2 (multiplets)	1.36, 1.32, 1.31 (dbs, 6.8 Hz)

[a] All spectra were run in CDCl$_3$ and shifts referenced to internal TMS standard.

Table IV. Infrared Data for Polyphosphoxane Complexes[a]

compd	CO stretch, cm^{-1}	POP stretch, cm^{-1}
1	2064, 1956, 1936, 1924	869
3	2003, 1925, 1923, 1900	833
4	2001, 1975, 1920, 1891	844
5	2011, 1961, 1936, 1915, 1883, 1871	890
6	2006, 1935, 1905, 1885	864
7	2014, 1913, 1896, 1886	839
8	2012, 1926, 1915, 1920	860
9		896
10		939

[a] KBr pellets.

to a *cis*-Cr(CO)$_4$ and a *fac*-Cr(CO)$_3$ unit to form a new type of bimetallic cage.

Tungsten hexacarbonyl also gave the monometallic product $W(CO)_4[{}^iPr_2NPO]_4$ after prolonged refluxing in toluene, again as a statistical mixture of two conformational isomers, **6a** and **6b** (30% yield).

Thermal reactions of other metal complexes such as $Fe(CO)_5$, $Fe_2(CO)_9$, $Ni(CO)_2(PPh_3)_2$, $[C_5H_5Fe(CO)_2]_2$, or $NiBr_2$·DME with the same phosphine oxide gave no tractable products. With $PdCl_2$ and $PdCl_2(PhCN)_2$, unstable O-coordinated products were obtained. Similarly, at room temperature, $Cr(CO)_5$·THF yielded an unstable O-bonded phosphine oxide complex which decomposed upon heating without rearranging to give P-coordinated products.

^{31}P NMR data of the described complexes are listed in Table I. ^{13}C and ^1H NMR data are presented in Tables II and III, respectively, while Table IV contains the infrared data.

Ligand Substitution Using the Triphosphoxane $[{}^iPr_2NPO]_3$. Direct room-temperature substitution by the triphosphoxane ring $[{}^iPr_2NPO]_3$ at metal centers containing labile ligands also yielded polyphosphoxane complexes. Only for Mo(CO)$_4$(norbornadiene) was the parent ring retained, giving a relatively unstable 1:1 complex *cis*-$Mo(CO)_4[{}^iPr_2NPO]_3$ (**7**) in about 60–70% yield (eq 3). This white solid also slowly transformed to the cage complex **2** upon standing at room temperature or warming in solution (eq 4).

$$\mathrm{Mo(CO)_4(NBD)} + [{}^i\mathrm{Pr_2NPO}]_3 \rightarrow \underset{\mathbf{7}}{\mathrm{Mo(CO)_4[{}^iPr_2NPO]_3}} + \mathrm{NBD} \quad (3)$$

$$2\underset{\mathbf{7}}{\mathrm{Mo(CO)_4[{}^iPr_2NPO]_3}} \rightarrow \underset{\mathbf{2}}{\mathrm{Mo_2(CO)_8[{}^iPr_2NPO]_4}} + 2[{}^i\mathrm{Pr_2NPO}] \quad (4)$$

The photochemical reaction of the triphosphoxane compound with Mo(CO)$_6$ gave a mixture of white monometallic $Mo(CO)_4[{}^iPr_2NPO]_4$ isomers **8a** and **8b** in about 20% yield as the major isolated products. An X-ray structural study revealed the presence of both species (Figures 4 and 5) in 1:2 statistical proportions, similar to the chromium and tungsten congeners, **3a**/**3b** and **6a**/**6b**. The thermal reaction, by contrast, gave a complex mixture of products, including cage **2** and intermediate **1**.

Both nickel(II) bromide and palladium(II) chloride yielded square-planar tetraphosphoxane complexes *cis*-$MX_2[{}^iPr_2NPO]_4$ when the appropriate solubilized dihalide complex was reacted with the triphosphoxane ring in hexane at room temperature (eqs 5 and 6). The palladium

$$3\mathrm{PdCl_2{\cdot}2PhCN} + 4[{}^i\mathrm{Pr_2NPO}]_3 \rightarrow 3\underset{\mathbf{9}}{\mathrm{PdCl_2[{}^iPr_2NPO]_4}} + 6\mathrm{PhCN} \quad (5)$$

$$3\mathrm{NiBr_2{\cdot}DME} + 4[{}^i\mathrm{Pr_2NPO}]_3 \rightarrow 3\underset{\mathbf{10}}{\mathrm{NiBr_2[{}^iPr_2NPO]_4}} + 3\mathrm{DME} \quad (6)$$

DME = dimethoxyethane

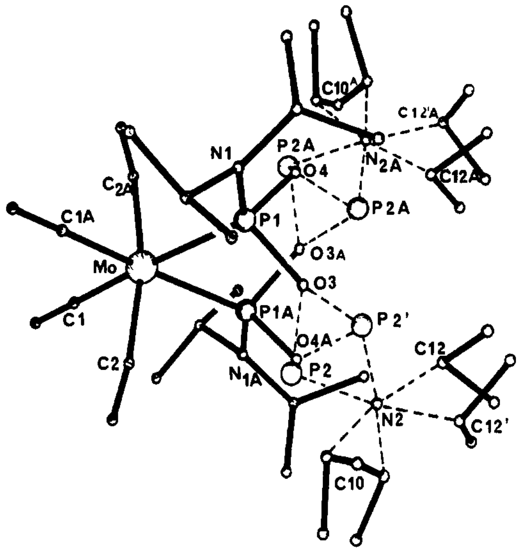

Figure 4. Molecular structure of Mo(CO)$_4$[^{i}Pr$_2$NPO]$_4$ (8). (Disordered sites are primed.)

reaction product, PdCl$_2$[^{i}Pr$_2$NPO]$_4$ (9), was isolated as a pale yellow solid in 40–50% yield. Its solution spectra and molecular structural determination confirmed the presence of only the chair–chair conformation of the 1,5-chelating P$_4$O$_4$ ring (Figure 6). A nickel analogue, NiBr$_2$[^{i}Pr$_2$NPO]$_4$, complex 10, is an orange-red solid obtained in about 60% yield. Its solution ^{31}P NMR spectrum is clearly dissimilar from that of 9, exhibiting an AA′XX′ instead of an A$_2$X$_2$ pattern (Figure 7), suggesting a fourth distinct coordination mode for the tetraphosphoxane ring. Similar results were obtained from NiCl$_2$·DME.

Release of the coordinated tetraphosphoxane [^{i}Pr$_2$NPO]$_4$ has been realized by pyridine displacement on the nickel bromide complex 10 at low temperature (−30 °C, chloroform-*d*; eq 7). The free ligand is stable at low temperature

$$\underset{10}{\mathrm{NiBr_2[{}^iPr_2NPO]_4}} + 2\mathrm{C_5H_5N} \rightarrow \mathrm{NiBr_2{\cdot}2C_5H_5N} + [{}^i\mathrm{Pr_2NPO}]_4 \quad (7)$$

$$3[{}^i\mathrm{Pr_2NPO}]_4 \rightarrow 4[{}^i\mathrm{Pr_2NPO}]_3 \quad (8)$$

and displays a singlet ^{31}P NMR signal at +130.7 ppm, suggesting either a static or averaged C_{4v} geometry for the uncomplexed P$_4$O$_4$ ring. This compound readily and irreversibly reverts to the triphosphoxane heterocycle upon warming in solution to room temperature (eq 8).

Discussion

Thermal Reaction of (^{i}Pr$_2$N)$_2$P(O)H with Metal Carbonyls. All three group VI metal hexacarbonyls reacted with the phosphine oxide upon heating in toluene to give complexes wherein carbonyls were replaced by cyclic trimeric, tetrameric, or pentameric phosphinidene oxide [^{i}Pr$_2$NPO]$_n$ ligands. Likely intermediates would contain the P-coordinated ^{i}Pr$_2$N—P=O unit, similar to the Cr(CO)$_5$[^{i}Pr$_2$NPO] complex reported by Niecke and co-workers.[7] A prime driving force for this and subsequent oligomerization steps must be the elimination of a bulky diisopropylamino group from the metal-coordinated phosphinous acid fragment (^{i}Pr$_2$N)$_2$P–OH (Scheme I). Use of the less hindered diethylamino group under the same reaction conditions led to little or no products of this type.[11] Further, the free phosphine oxide underwent no perceptible reaction in the absence of metal carbonyls. The milder reaction conditions for Mo(CO)$_6$ allowed the isolation and characterization of one intermediate, the triphosphoxane complex 1, Mo(CO)$_5$[^{i}Pr$_2$NPO]$_3$. A ^{31}P NMR spectrum of the reaction mixture after 4–5 h at 100 °C revealed unsubstituted phosphine oxide and the AMX pattern of 1 as well as a small amount of an AX$_2$ species that may be an isomer of 1. Upon reflux of the mixture in toluene, these readily transformed to the thermodynamic product, a bimetallic cage complex 2, which contains the P$_4$O$_4$ heterocycle as a boat–boat tetradentate donor (structure type A in Figure 1).[8] The even more facile conversion of Mo(CO)$_4$[^{i}Pr$_2$NPO]$_3$ (7) to the same complex 2 indicates that more than one intermediate can lead to the same thermodynamic cage product (Scheme II). Interestingly, the kinetically more sluggish Cr(CO)$_6$ and

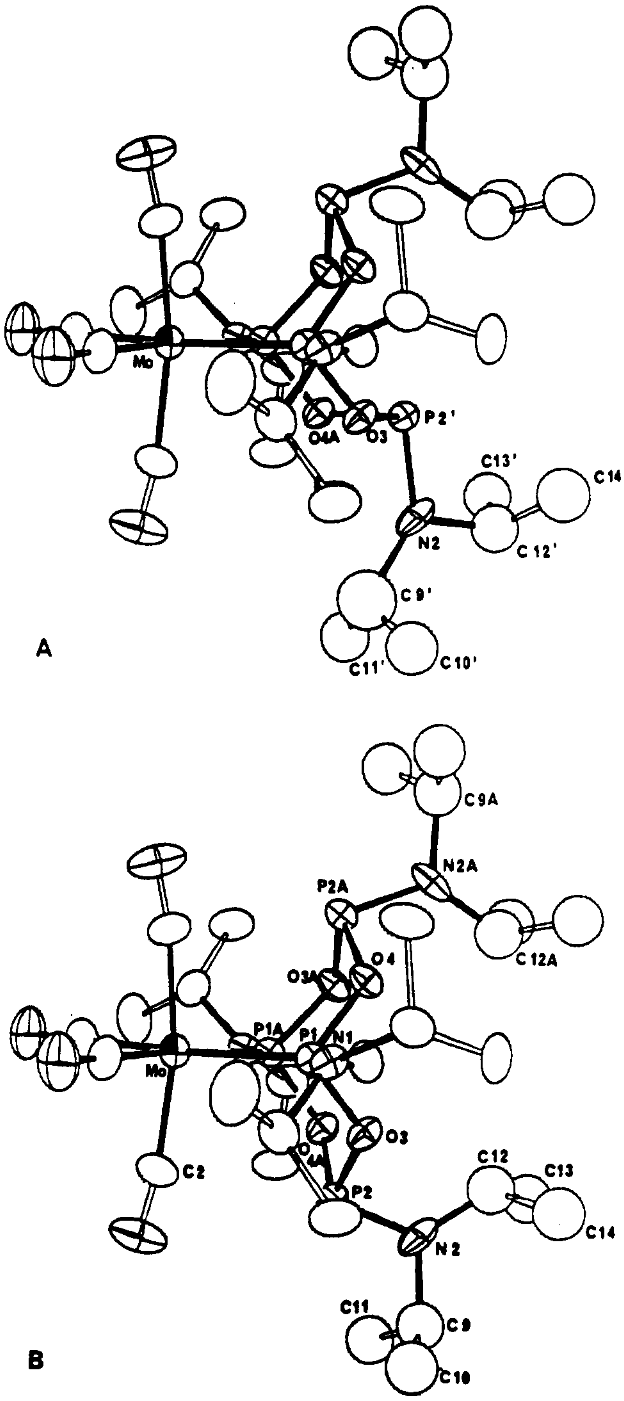

Figure 5. (A) Molecular structure of 8a, the chair–boat form, and (B) molecular structure of 8b, the chair–chair form.

---

[11] Private communication: Prof. M. M. Turnbull of Clark University has prepared the corresponding diethylamino cage complex in fair yield by using different reaction conditions.

Scheme I

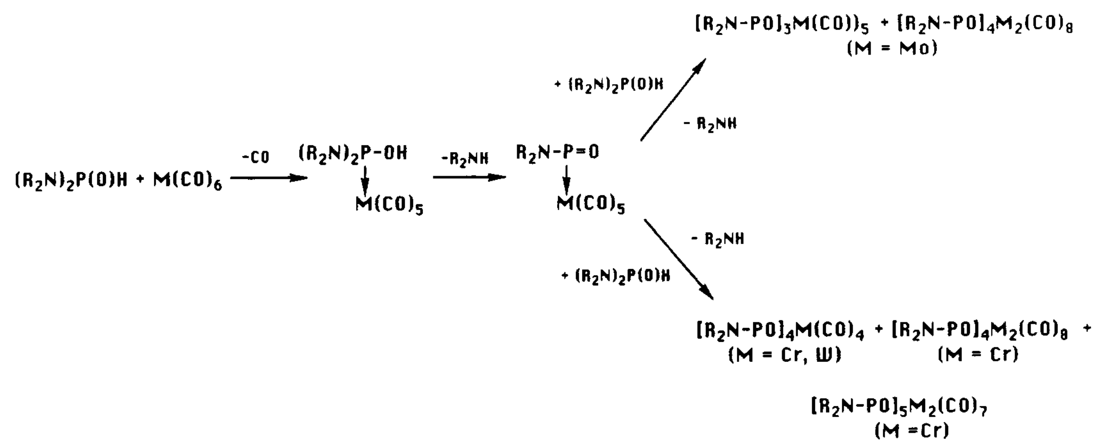

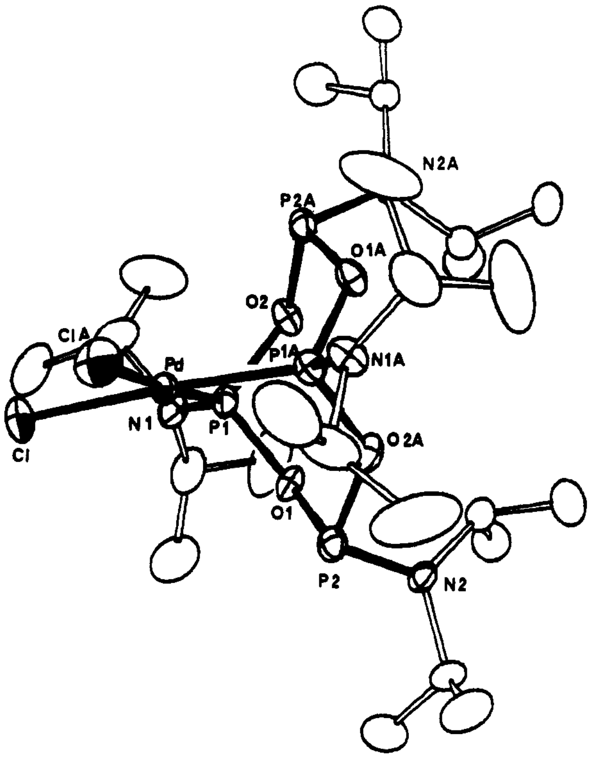

Figure 6. Molecular structure of 9.

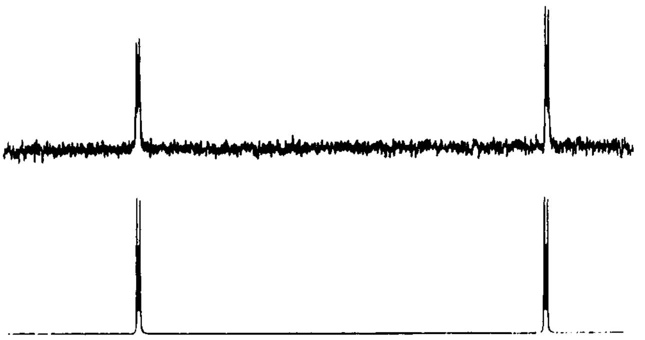

Figure 7. ^{31}P NMR spectrum of $NiBr_2[^iPr_2NPO]_4$ (10) (top trace) and a simulation (bottom trace) of the AA'XX' pattern with $J_{AX} = J_{A'X'} = 20$ Hz and $J_{AX'} = J_{A'X} = 1$ Hz.

$W(CO)_6$ failed to give cage analogues in similar reactions. It appears that only the fortuitous combination of Mo and this particular phosphinidene oxide can lead to that structural type.

By contrast, the major Cr and W products are monometallic *cis*-$M(CO)_4[^iPr_2NPO]_4$ isomers, **3a**/**3b** and **6a**/**6b**,

Scheme II

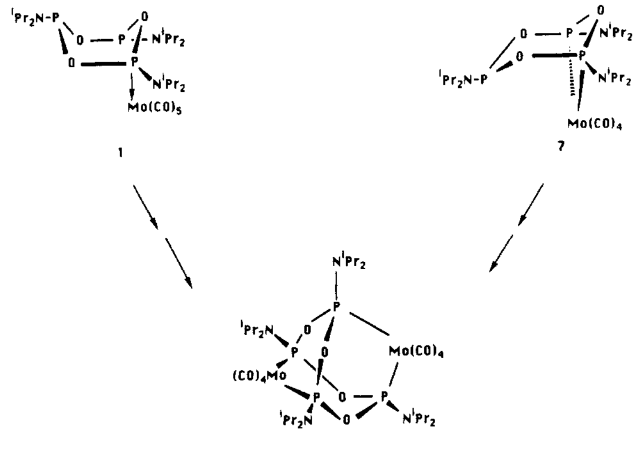

1

7

2

Scheme III

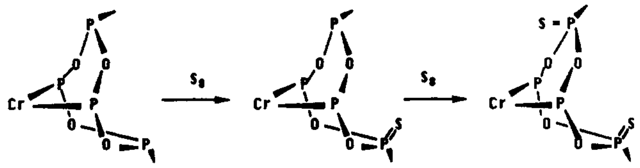

3b

12

13

respectively, featuring the tetraphosphoxane ring as a 1,5-chelating ligand. Their similar IR and NMR spectral data and the X-ray structural determination of their molybdenum analogues **8a**/**8b** are fully consistent with the formation of 1:2 statistical mixtures of the chair–chair and chair–boat conformations of the P_4O_4 ring. A substantial barrier to phosphorus inversion can be gauged from the temperature-independent NMR spectral behavior up to 110 °C. Unlike **1** or **7**, all these compounds are quite robust and do not show any tendency to transform to the corresponding cage species. For example, heating of **8a**/**8b** alone or with $Mo(CO)_6$ failed to produce **2**.

One of the uncoordinated P atoms in the complexes **3b**, **6b**, and **8b** appears to be sterically blocked from further coordination. For instance, reaction of **3b** with excess $Cr(CO)_5$·THF gave a 1:1 complex only. Assuming that phosphorus inversion is not occurring, access to the free phosphorus atom in the chair part of P_4O_4 ring must be hindered by the axial metal carbonyl. Similarly, reactions with sulfur resulted in ready sulfurization of the accessible boat-phosphorus atom of the chair–boat conformer to give complex **12**, while the remaining site only sulfurized after

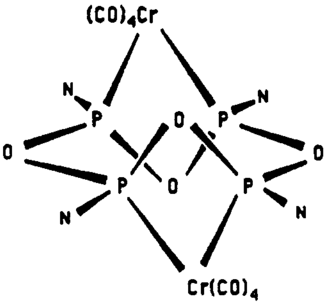

Figure 8. Proposed structure for complex 4.

prolonged reaction times to give $Cr(CO)_4[^iPr_2NPO]_4S_2$, complex 13 (Scheme III).

The thermal reaction of $Cr(CO)_6$ with $(^iPr_2N)_2P(O)H$ also produced a minor amount of $Cr_2(CO)_8[^iPr_2NPO]_4$, light yellow complex 4. Its composition was confirmed by elemental analyses and a cryoscopic molecular weight determination. The structure of 4 can be deduced from its ^1H, ^{13}C and ^{31}P NMR spectra, which are consistent with a bimetallic complex of the tetraphosphoxane ring. Models suggest that a twist-boat/twist-boat (C_i) conformation is most likely (Figure 8). This can also be viewed as two *cis*-$Cr(CO)_4$(P–O–P) chelate rings linked by an additional pair of P–O–P bonds. If confirmed, this will represent a constitutional isomer of the still unknown chromium analogue of cage complex 2. The smaller chromium atom appears to be able to adapt comfortably into the four-membered Cr–P–O–P chelate ring under these reaction conditions.

Prolonged reaction times of 60 h or more gave instead of 4 small yields of the yellow complex 5, characterized as the pentaphosphoxane complex $Cr_2(CO)_7[^iPr_2NPO]_5$. The P_5O_5 ring incorporated into this species is novel (structure type B, Figure 1). Again, a four-membered Cr–P–O–P chelate ring is featured. This cage complex has also been synthesized recently in good yields by Turnbull and coworkers using even more rigorous reaction conditions.[12] The absence of any dichromium P_4O_4 cage product (type A in Figure 1) and the subsequent formation of this larger dichromium P_5O_5 cage complex 5 under more severe conditions underscore a basic size mismatch between the chromium tetracarbonyl moiety and the boat–boat P_4O_4 ring found in a type A structure.

Ligand Substitution Using the Triphosphoxane $[^iPr_2NPO]_3$. Direct substitution by the triphosphoxane P_3O_3 ring yielded different results from the phosphine oxide reactions. Thermal reaction with $Mo(CO)_6$ gave a complex mixture of intermediate 1 and cage 2 as well as other uncharacterized species. By contrast, the photochemical reaction afforded a fair yield of the 1,5-P_4O_4-coordinated products $Mo(CO)_4[^iPr_2NPO]_4$ (**8a**/**8b**), the Mo analogues of **3a**/**3b** and **6a**/**6b**. Interestingly, only traces of the cage complex 2 so heavily favored in the phosphine oxide thermal reactions was found. Like **3a**/**3b** and **6a**/**6b**, **8a**/**8b** showed no tendency to transform into bimetallic cages of type A (Figure 1).

Formation of complex 9, $PdCl_2[^iPr_2NPO]_4$, from the triphosphoxane compound and $PdCl_2(PhCN)_2$ in a room-temperature reaction illustrates the ease of metal-induced trimer/tetramer equilibration. Possibly due to the lack of axial steric encumbrance in a square-planar geometry, only the chair–chair conformation is observed both in solution and the solid state (Figure 6).

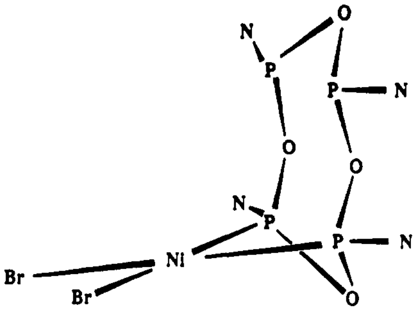

Figure 9. Proposed structure for complex 10.

Scheme IV

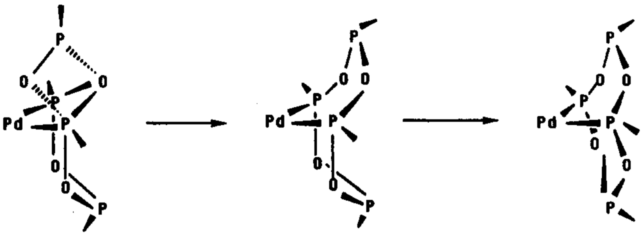

The formation of such a tetraphosphoxane complex from a triphosphoxane ring at ambient temperature requires incorporation of an additional phosphinidene oxide unit as well as a phosphorus inversion at one of the original ring phosphorus atoms. One can speculate that coordination of the P_3O_3 ring to Pd(II) occurs initially. Assuming a small but finite concentration of the phosphinidene oxide monomer in equilibrium with the trimer, this can insert in a head-to-tail manner at a P–O ring bond (Scheme IV). For Pd(II), the isnertion must occur at a coordinated ring phosphorus atom. Considering the mild reaction conditions, the P inversion step can only be feasible if an original ring $^iPr_2N$—P=O unit eliminates and subsequently readds from a new orientation. Another plausible mechanism is for Pd(II) to coordinate to monomeric or dimeric $[^iPr_2N-PO]_n$ units, which subsequently build up to the final P_4O_4 complex.

The $NiBr_2$ and $NiCl_2$ products (complexes 10 and 11) are also 1:1 complexes of tetraphosphoxane. However, their ^{31}P NMR spectra were clearly AA′XX′ (Figure 7) instead of A_2X_2, and their structures can be unambiguously assigned to contain the 1,3-chelating (Figure 9) rather than the 1,5-chelating P_4O_4 ring ($J_{AX} = J_{A'X'} \neq J_{AX'} = J_{A'X}$). Like the Cr complexes 4 and 5 discussed above, the preference of a smaller Ni(II) center for a four-membered chelate ring may also explain the adoption of this disparate coordination mode.

^{31}P NMR Spectra. Proton-decoupled ^{31}P NMR spectroscopy provided firm structural assignments for many of the products. For the triphosphoxane complex 1, an AMX pattern for $Mo(CO)_5[^iPr_2NPO]_3$ suggested monodentate complexation at one of the two formerly equivalent phosphorus atoms. A reasonable coordination shift of +17 ppm at the coordinated ^{31}P nucleus is observed.[4,13]

For the $M(CO)_4[^iPr_2NPO]_4$ products, A_2X_2 (**3b**, **6b**) or AA′XX′ (**8b**) patterns were observed for the chair–chair conformers. The noncoordinated P nuclei can be readily assigned to the multiplets at 143–148 ppm. Observed coordinated P shifts at 173, 150, and 126 ppm for Cr, Mo, and W, respectively, are in accord with expected coordination shifts for phosphine complexes of this triad.[13] The

---

[12] Banse, C. M.; Pray, M. A.; Turnbull, M. M. *Polyhedron* **1989**, *8*, 2719–2721.

[13] Pregosin, P. S.; Kunz, R. W. *^{31}P and ^{13}C NMR of Transition Metal Phosphine Complexes*; Springer-Verlag: Berlin, 1979. Pregosin, P. S. *P-31 NMR Spectroscopy in Stereochemical Analysis*; Verkade, J. G., Quin, L. D., Eds.; VCH: Weinheim, Germany, 1987; pp 500–501.

$^1J_{W-P}$ coupling constant of 166 Hz is also reasonable. For Mo and Cr, first-order A_2XY patterns were clearly observed for the boat-chair form (**8a** and **3a**). Assignments of the A_2 part of each spectrum to the coordinated P atoms can be readily made. For both, δ_X = 129 and δ_Y = 127 ppm. In the W analogue **6a**, a second-order AB_2X pattern appeared with the coordinated P atoms assignable to the B_2 portion at δ = 133 ppm and with $^1J_{W-P}$ of 167 Hz. Consistent with expected high phosphorus inversion barriers, no significant changes in these solution spectra occurred upon heating to 110 °C.

Complex **4**, with a molecular formula of $Cr_2(CO)_8[^iPr_2NPO]_4$ and a singlet ^{31}P NMR chemical shift at +159.4 ppm, is significantly shifted upfield compared to the +177.4 ppm observed for the coordinated P atoms in complex **3a**, *cis*-$Cr(CO)_4[^iPr_2NPO]_4$. Both the proton and ^{13}C spectra revealed two distinct diastereotopic methyls for the isopropyl groups. These spectra suggest a lack of symmetry above and below the *cis*-CrP_2 chelate plane. A reasonable structure would have a tetradentate P_4O_4 ring in a twist-boat/twist-boat (C_i) conformation 1,3- and 5,7-coordinated to two $Cr(CO)_4$ moieties (Figure 8). The resulting linked four-membered Cr-P-O-P chelate rings can account for the −18 ppm upfield shift (the "ring contribution")[14] of the ^{31}P signal in **4** compared to **3a** as well as the diastereotopic methyl ^{13}C and ^1H NMR signals.

For the dichromium pentaphosphoxane complex **5**, an A_2MX_2 spectrum was found. Assuming that the solid-state structure is retained in solution and the high-field multiplet is from the four-membered chelate ring, we can assign the MX_2 portion of the spectrum to the *fac*-$Cr(CO)_3$ P atoms and the A_2 resonances to the *cis*-$Cr(CO)_4$ P atoms.

Complex **7** displayed an A_2X spectrum consistent with its proposed structure featuring a symmetrically coordinated P_3O_3 ring in either the boat or chair conformation. The coordination shift of only +7 ppm is consistent with the ring contribution due to the formation of a four-membered chelate ring.[14] We favor the chair form, since the upfield shift of the free P from 140.3 to 130.1 ppm upon coordination can be a result of the P_3O_3 ring flipping into a chair conformation. This will relieve the postulated transannular P- - -O interaction in the boat form of the parent heterocycle, causing an upfield shift for this nucleus.[4]

Proton and ^{13}C NMR Spectra. All complexes displayed proton NMR spectra featuring the isopropyl methine groups as septets in the 3.5–4.2 ppm region and methyl groups as doublets in the 1.1–1.4 ppm range having $^3J_{H-H}$ couplings of 6–7 Hz.

The ^{13}C NMR data showed isopropyl methyl carbons in the 22–25 ppm region and methine carbons in the 45–49 ppm range. The latter usually displayed $^2J_{C-P}$ couplings of 3–6 Hz. Carbonyl carbon spectra were useful in assigning coordination structures. For example, complex **1**'s spectrum contained a doublet at 210.6 ppm with a P-C coupling of 39 Hz and a larger doublet of doublets at 205.7 (J's = 4 and 13 Hz). The former pattern can be readily assigned to the lone CO group trans to the P ligand, and the latter, to the four equatorial CO's ($^2J_{C-P(1)}$ = 13 Hz and $^4J_{C-P(2)\text{ or }P(3)}$ = 4 Hz). Carbonyl ^{13}C's in complex **4** supported the asymmetry of the two axial CO's (six peaks). The low symmetry of the dichromium complex **7** can also be deduced from the five observed CO multiplets between 230 and 216 ppm.

X-ray Structural Data. Crystal Structure of $Mo(CO)_5[^iPr_2NPO]_3$ (1). The molecular structure of complex **2** can be compared to that of the parent ring previously reported by Niecke et al.[4] Both show a boat conformation with only small changes in ring angles and bond distances upon metal coordination. The transannular P(3)- - -O(6) distance is slightly elongated to 3.23 Å from 3.01 Å. The O-P-O and O-P-N angles around P(1) also opened up slightly from 97–101 to 100–110° upon Mo bonding. All three diisopropylamino groups remain equatorial with the metal moiety axial. The geometry around the molybdenum coordination sphere is unexceptional. Relevant bond distances and angles are listed in Table V.

Table V. Selected Bond Distances (Å) and Angles (deg) for 1[a]

Mo-P(1)	2.513 (3)	P(1)-N(1)	1.636 (11)
Mo-C(1)	2.002 (16)	P(2)-O(6)	1.702 (9)
Mo-C(2)	2.028 (15)	P(2)-O(7)	1.681 (10)
Mo-C(3)	2.005 (17)	P(2)-N(2)	1.663 (11)
Mo-C(4)	2.020 (15)	P(3)-O(7)	1.622 (11)
Mo-C(5)	1.951 (15)	P(3)-O(8)	1.704 (9)
P(1)-O(6)	1.637 (9)	P(3)-N(3)	1.641 (12)
P(1)-O(8)	1.617 (9)		

P(1)-Mo-C(1)	174.5 (6)	P(1)-O(6)-P(2)	121.0 (5)
Mo-P(1)-O(6)	114.0 (3)	P(2)-O(7)-P(3)	128.6 (6)
Mo-P(1)-O(8)	110.0 (3)	P(1)-O(8)-P(3)	123.5 (5)
Mo-P(1)-N(1)	121.7 (4)	O(6)-P(2)-O(7)	94.0 (5)
O(6)-P(1)-O(8)	100.3 (4)	O(6)-P(2)-N(2)	99.1 (5)
O(6)-P(1)-N(1)	103.9 (5)	O(7)-P(2)-N(2)	104.1 (6)
O(8)-P(1)-N(1)	104.4 (5)	O(7)-P(3)-O(8)	96.9 (5)
O(7)-P(3)-N(3)	103.6 (6)	O(8)-P(3)-N(3)	98.5 (6)

[a] Estimated standard deviations are in parentheses.

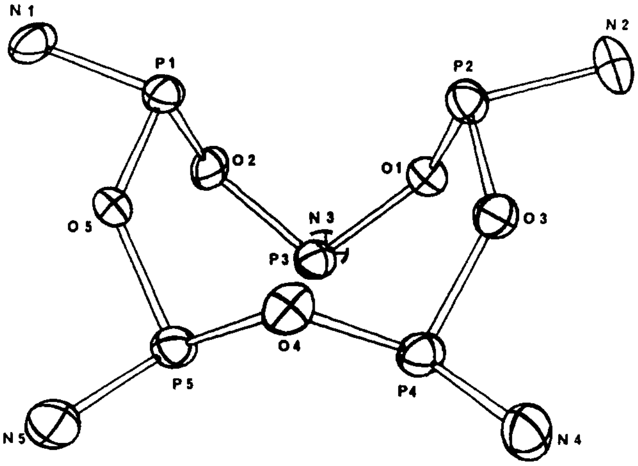

Figure 10. Conformation of the P_5O_5 ring in complex **5**. Cr(1) is coordinated to P(1) and P(2), while Cr(2) is coordinated to P(3), P(4), and P(5).

Crystal Structure of $Cr_2(CO)_7[^iPr_2NPO]_5$ (5). The conformation of the 10-membered pentaphosphoxane ring set up to complex both the *cis*-$Cr(CO)_4$ and *fac*-$Cr(CO)_3$ units is shown in Figure 10. There is an approximate mirror plane containing O(4) and P(3) that bisects the P_5O_5 ring. The four-membered chelate ring made up of Cr(2), P(4), O(4), and P(5) is planar to within 0.056 Å and contains a small P-O-P angle of 101.0 (5)° as well as an unusually compressed P-Cr-P angle of 66.4 (2)° (Figure 3).[15] Atoms P(4) and P(5) in this heterocycle are 2.533 (5) Å apart, only about 0.2 Å longer than typical P-P single bond distances. The bond-angle sums around all five amino nitrogens are within 2° of planarity (360°). Relevant bond distances and angles are listed in Table VI. The conformational flexibility we have found in the coordination

---

(14) Garrou, P. E. *Chem. Rev.* **1981**, *81*, 229–266.

(15) Wong, E. H.; Prasad, L.; Gabe, E. J.; Bradley, F. C. *J. Organomet. Chem.* **1982**, *236*, 321–331.

Table VI. Selected Bond Distances (Å) and Angles (deg) for 5[a]

Cr(1)–P(1)	2.352 (4)	P(1)–O(5)	1.626 (10)
Cr(2)–P(2)	2.336 (5)	P(2)–O(1)	1.643 (9)
Cr(1)–C(1)	1.865 (18)	P(2)–O(3)	1.621 (10)
Cr(1)–C(2)	1.859 (15)	P(2)–N(2)	1.688 (11)
Cr(1)–C(3)	1.860 (18)	P(3)–O(1)	1.643 (8)
Cr(1)–C(4)	1.860 (17)	P(3)–O(2)	1.640 (9)
Cr(2)–P(3)	2.288 (5)	P(3)–N(3)	1.672 (12)
Cr(2)–P(4)	2.315 (4)	P(4)- - -P(5)	2.533 (5)
Cr(2)–P(5)	2.312 (5)	P(4)–O(3)	1.649 (9)
Cr(2)–C(5)	1.829 (17)	P(4)–O(4)	1.648 (9)
Cr(2)–C(6)	1.823 (17)	P(4)–N(4)	1.649 (13)
Cr(2)–C(7)	1.878 (15)	P(5)–O(4)	1.635 (9)
P(1)–O(2)	1.639 (9)	P(5)–O(5)	1.644 (10)

P(1)–Cr(1)–P(2)	89.29 (15)	P(3)–Cr(2)–P(4)	92.25 (16)
P(1)–Cr(1)–C(1)	89.2 (5)	P(3)–Cr(2)–P(5)	91.11 (16)
P(1)–Cr(1)–C(2)	176.4 (5)	P(3)–Cr(2)–C(5)	176.5 (5)
P(1)–Cr(1)–C(3)	93.7 (5)	P(3)–Cr(2)–C(6)	88.6 (6)
P(1)–Cr(1)–C(4)	89.8 (5)	P(3)–Cr(2)–C(7)	90.0 (5)
P(2)–Cr(1)–C(1)	88.8 (5)	P(4)–Cr(2)–P(5)	66.37 (15)
P(2)–Cr(1)–C(2)	93.3 (5)	P(4)–Cr(2)–C(5)	90.7 (5)
P(2)–Cr(1)–C(3)	91.4 (5)	P(4)–Cr(2)–C(6)	99.5 (5)
P(2)–Cr(1)–C(4)	177.4 (6)	P(4)–Cr(2)–C(7)	164.5 (5)
C(1)–Cr(1)–C(2)	93.5 (7)	P(5)–Cr(2)–C(5)	91.9 (5)
C(1)–Cr(1)–C(3)	177.1 (7)	P(5)–Cr(2)–C(6)	165.8 (5)
C(1)–Cr(1)–C(4)	93.6 (8)	P(5)–Cr(2)–C(7)	98.2 (5)
C(2)–Cr(1)–C(3)	83.6 (7)	C(5)–Cr(2)–C(6)	88.9 (8)
C(2)–Cr(1)–C(4)	87.6 (6)	C(5)–Cr(2)–C(7)	87.7 (7)
C(3)–Cr(1)–C(4)	86.3 (8)	C(6)–Cr(2)–C(7)	95.9 (7)
P(4)–O(4)–P(5)	101.0 (5)		

[a] Estimated standard deviations are in parentheses.

Table VII. Selected Bond Distances (Å) and Angles (deg) for 8[a]

Mo–P(1)	2.4923 (24)	P(2)–O(4A)	1.715 (6)
Mo–C(1)	1.978 (9)	P(2)–N(2)	1.666 (8)
Mo–C(2)	2.007 (9)	P(2′)–O(3)	1.718 (9)
P(1)–O(3)	1.634 (5)	P(2′)–O(4A)	1.701 (9)
P(1)–O(4)	1.607 (6)	P(2′)–N(2)	1.739 (11)
P(1)–N(1)	1.660 (6)	O(1)–C(1)	1.156 (11)
P(2)–O(3)	1.669 (6)	O(2)–C(2)	1.144 (11)

P(1)–Mo–P(1A)	76.18 (8)	O(3)–P(1)–O(4)	99.6 (3)
P(1)–Mo–C(1)	172.3 (3)	O(3)–P(1)–N(1)	104.0 (3)
P(1)–Mo–C(1A)	96.8 (3)	O(4)–P(1)–N(1)	100.8 (3)
P(1)–Mo–C(2)	98.1 (3)	O(3)–P(2)–O(4A)	94.9 (3)
P(1)–Mo–C(2A)	90.8 (3)	O(3)–P(2)–N(2)	99.1 (4)
C(1)–Mo–C(1A)	90.4 (4)	O(4A)–P(2)–N(2)	98.6 (4)
C(1)–Mo–C(2)	85.1 (4)	O(3)–P(2′)–O(4A)	93.7 (4)
C(1)–Mo–C(2A)	87.0 (4)	O(3)–P(2′)–N(2)	94.5 (5)
C(2)–Mo–C(2A)	168.7 (4)	P(1)–O(4)–P(2′A)	121.6 (4)
Mo–P(1)–O(3)	112.1 (2)	O(4A)–P(2′)–N(2)	96.4 (5)
Mo–P(1)–O(4)	112.1 (2)	P(1)–O(3)–P(2)	125.3 (3)
Mo–P(1)–N(1)	124.9 (3)	P(1)–O(3)–P(2′)	127.1 (4)

[a] Estimated standard deviations are in parentheses.

Table VIII. Selected Bond Distances (Å) and Angles (deg) for 9[a]

Pd–Cl	2.3457 (17)	P(1)–N(1)	1.621 (5)
Pd–P(1)	2.2483 (15)	P(2)–O(1)	1.663 (4)
P(1)–O(1)	1.617 (4)	P(2)–O(2A)	1.686 (4)
P(1)–O(2)	1.592 (4)	P(2)–N(2)	1.630 (4)

Cl–Pd–Cl(A)	89.69 (8)	P(1)–O(2)–P(2A)	124.47 (23)
Cl–Pd–P(1)	93.04 (6)	O(1)–P(1)–O(2)	102.72 (21)
Cl–Pd–P(1A)	175.80 (7)	O(1)–P(1)–N(1)	105.41 (23)
P(1)–Pd–P(1A)	84.41 (6)	O(2)–P(1)–N(1)	102.76 (24)
Pd–P(1)–O(1)	107.88 (16)	O(1)–P(2)–O(2A)	96.24 (20)
Pd–P(1)–O(2)	111.16 (14)	O(1)–P(2)–N(2)	99.84 (20)
P(1)–O(1)–P(2)	128.59 (24)	O(2A)–P(2)–N(2)	99.54 (20)

[a] Estimated standard deviations are in parentheses.

modes of the tetraphosphoxane ring may well be shared by the P_5O_5 heterocycle in its largely unexplored coordination chemistry.

Crystal Structure of $Mo(CO)_4[^iPr_2NPO]_4$ (8). The molecular structures of both **8a** and **8b** can be deduced from the disordered structure shown in Figure 4. A 2-fold symmetry axis through the metal center correlates the two halves of the coordination sphere. The disorder involves only the uncoordinated phosphorus atoms and their associated diisopropyl groups. To better visualize the disorder, one can imagine a phosphorus inversion at P(2) anchored at ring oxygen atoms O(3), O(4A), and N(2) in **8b** (Figure 5B) to bring it from the chair conformation into the boat form at P(2′) in **8a** (Figure 5A). C(9)–C(14) will similarly be transposed into new positions C(9′)–C(14′), respectively. The occupanices of the primed and unprimed sites are 1:2, respectively, in accordance with the spectral data of single crystals indicating a statistical mixture of chair–chair and chair–boat forms. The former ring is considerably flattened (Figure 5B) as the uncoordinated P(2) and P(2A) are bent away from the axial metal carbonyls to within 0.1 Å of the ring oxygen plane (O(3), O(3A), O(4), O(4A)). In fact, the P(2)- - -C(2) contact is 0.5 Å below their van der Waals radii sum. Similarly, the axial carbonyl–metal–carbonyl angle is compressed from linearity to 168.7 (4)°. Important bond angles and distances are listed in Table VII.

Crystal Structure of $PdCl_2[^iPr_2NPO]_4$ (9). Relevant bond distances and angles are listed in Table VIII. The molecule contains a crystallographic 2-fold axis through palladium that relates the two halves of the $[^iPr_2NPO]_4$ heterocycle (Figure 6). The coordination geometry around Pd(II) is essentially planar (bond angles sum to 360.2°). Bond distances and angles are typical of *cis*-dichloropalladium diphosphine complexes.[16] The tetraphosphoxane ring is found to coordinate as a 1,5-chelator exclusively in the chair–chair conformation. As in complex **8a**, the ring is considerably flattened with P(2) and P(2A) only 0.01 Å out of the O(1), O(1A), O(2), O(2A) plane. Unlike **8a**, however, there are no axial ligands on the metal to account for this flattening, nor did examination of the diisopropylamino substituents reveal any unusual steric problems. Such a distortion of the P_4O_4 ring may be an inherent consequence of its 1,5-chelating mode, which brings P(1) and P(1A) toward the metal while pushing P(2) and P(2A) away into the ring oxygens' plane.

Conclusions

The thermal reaction of $(^iPr_2N)_2P(O)H$ with group VI metal carbonyls and direct substitution of $[^iPr_2NPO]_3$ at metal centers for labile ligands provide two approaches to the syntheses of polyphosphoxane complexes. X-ray structural data as well as solution NMR spectra show that the tetraphosphoxane $[^iPr_2NPO]_4$ ring is unusually versatile in its coordinative and conformational flexibility (Figure 11). It can be a 1,3,5,7-tetradentate ligand adopting a boat–boat conformation in bimetallic cage complexes or an isomeric open structure with the P_4O_4 ring in a C_i geometry. It can also function as a 1,5-bidentate donor toward a single metal center, adopting either a chair–boat or chair–chair form. Additionally, a 1,3-chelating mode is also feasible for smaller metals.

The triphosphoxane $[^iPr_2NPO]_3$ behaves as a mono- or bidentate ligand, yielding significantly less robust products that readily transform into the tetraphosphoxane cage complex. By contrast, as the free ligand, tetraphosphoxane

---

[16] Corbridge, D. E. C. *The Structural Chemistry of Phosphorus*; Elsevier: New York, 1974; 302. Gramlich, V.; Consiglio, G. *Helv. Chim. Acta* **1979**, *62*, 1016–1024.

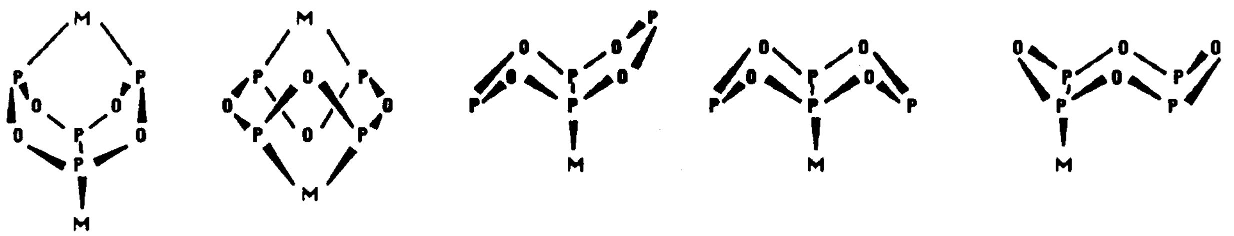

Figure 11. The five possible coordination modes of the P_4O_4 tetraphosphoxane.

is unstable relative to triphosphoxane, reverting to it under ambient conditions.

The novel pentaphosphoxane $[^iPr_2NPO]_5$ ring was formed around two chromiums. Structural characterization confirmed that it can serve as a pentadentate ligand simultaneously toward one cis- and one *fac*-coordinated metal.

Our isolation of these polyphosphoxane complexes further demonstrates the unique ability of metal coordination to provide superstructures for novel ring and cage systems.[17] We hope to exploit their chemistry and suitability as precursors to new heterometallic complexes.

Experimental Section

All manipulations were carried out by using standard Schlenk techniques under an atmosphere of prepurified nitrogen. Hexane was distilled from CaH_2 and toluene from sodium, while THF was distilled from sodium benzophenone ketyl. Diisopropylamine and phosphorus trichloride were purchased from Aldrich Chemicals. Triethylamine was distilled from KOH before use. Sodium hydride as a 50% dispersion in oil was from Alfa Chemical Co. The metal hexacarbonyls were purchased from Pressure Chemicals, Inc. Bis(diisopropylamine) oxide,[8] (norbornadiene)molybdenum tetracarbonyl,[18] bis(benzonitrile)palladium dichloride,[19] and nickel dibromide–dimethoxyethane[20] were prepared according to literature procedures. ^1H, ^{13}C, and ^{31}P NMR spectra were recorded on both JEOL FX90Q and Bruker AM360 spectrometers using an internal deuterium lock. ^1H and ^{13}C shifts were referenced to internal TMS, while ^{31}P shifts were referenced to external 85% phosphoric acid. Infrared spectra were recorded on a Perkin-Elmer 283B instrument. IR data for the complexes are listed in Table IV. A Hanovia 450-W medium-pressure mercury lamp in a quartz immersion well was used for the photoreaction. Elemental analyses were performed at the University of New Hampshire Instrumentation Center with a Perkin-Elmer 240B elemental analyzer.

$Mo(CO)_5[^iPr_2NPO]_3$ (1). In a 50-mL flask, 4.00 g (16.2 mmol) of bis(diisopropylamino)phosphine oxide and 2.4 g (9.1 mmol) of $Mo(CO)_6$ in 20 mL of toluene were heated in an oil bath at 100 °C for 4–5 h. After cooling, the yellow solution with white $Mo(CO)_6$ precipitate was concentrated under reduced pressure to about 10 mL and filtered. The filtrate was evaporated to a viscous oil, which was dissolved in 10 mL of methylene chloride and deposited onto about 10 g of alumina (neutral, Brockman I grade). After evaporation, the light yellow residue was extracted with 10 mL of hexane and filtered. The light yellow filtrate was evaporated and the residue chromatographed on a 2 × 15 cm column of alumina (same grade) using hexane as the eluant. The first fraction to elute was crude complex 1. After evaporation, the white solid was recrystallized from cold hexane to give ~200 mg (5% yield from the phosphine oxide) of 1. Anal. Calcd for $C_{23}H_{42}MoN_3O_8P_3$: N, 6.20; C, 40.80; H, 6.20. Found: N, 6.31; C, 40.91; H, 6.59.

Thermolysis of Complex 1. A 50-mg sample of 1 was dissolved in 1 mL of toluene in a Schlenk tube and refluxed for 1.5 h. TLC indicated only cage complex 2. This was confirmed by ^{31}P NMR spectroscopy as well as workup of the evaporated residue by chromatography on a silica gel column and isolation of 2 as a white solid in about 80% yield.

$Cr(CO)_4[^iPr_2NPO]_4$ (3a,b) and $Cr_2(CO)_8[^iPr_2NPO]_4$ (4). The phosphine oxide (10.0 g, 40.5 mmol) and 5.00 g (22.7 mmol) of $Cr(CO)_6$ were refluxed in 70 mL of toluene for about 48 h. After evaporation of the volatiles under reduced pressure, the dark brown residue was extracted with 20 mL of acetone and the solution filtered to give an off-white crystalline solid. This was recrystallized twice from hot hexane to give large clear crystals of 3 and small light yellow crystals of 4. These were readily separated manually to give the pure products. Typical yields based on the phosphine oxide are 30% (2.3 g) and 2% (200 mg) for 3 and 4, respectively. Anal. Calcd for $C_{28}CrH_{56}N_4O_8P_4$: N, 7.42; C, 44.53; H, 7.42. Found: N, 7.39; C, 44.85; H, 7.77. Calcd for $C_{32}H_{56}Cr_2N_4O_{12}P_4$: N, 6.11; C, 41.92; H, 6.11. Found: N, 5.91; C, 41.90; H, 6.02.

$Cr_2(CO)_7[^iPr_2NPO]_5$ (5). The phosphine oxide (10.0 g, 40.5 mmol) and and 5.00 g (22.7 mmol) of $Cr(CO)_6$ were refluxed in 70 mL of toluene for about 90 h. The volatiles were removed under reduced pressure and the residue extracted with 20 mL of acetone to give white crystalline complex 3 upon filtration. The filtrate was concentrated to about 10 mL to precipitate more 3 and again filtered. The filtrate was evaporated to dryness and the residue recrystallized from hot hexane to give large yellow crystals of complex 5 in about 5% yield based on the phosphine oxide, 400–500 mg. Anal. Calcd for $C_{37}Cr_2H_{70}N_5O_{12}P_5$: N, 6.76; C, 42.90; H, 6.76. Found: N, 6.44; C, 42.88; H, 7.04.

$W(CO)_4[^iPr_2NPO]_4$ (6a,b). The phosphine oxide (4.20 g, 17.0 mmol) and 3.0 g (8.5 mmol) of $W(CO)_6$ were refluxed in 20 mL of toluene for about 40 h. After evaporation of the volatiles, the residue was extracted with 10 mL of methylene chloride and the solution filtered to remove insoluble $W(CO)_6$. The filtrate was evaporated to dryness and extracted with 5 mL of acetone. Filtration and washing of the residue with cold acetone gave a 30% yield (1.1 g) of complex 6 as a white, crystalline solid. Recrystallization from hot hexane afforded large clear crystals. Anal. Calcd for $C_{28}H_{56}N_4O_8P_4W$: N, 6.33; C, 38.04; H, 6.33. Found: N, 6.47; C, 38.27; H, 6.43.

$(^iPr_2N)PCl_2$, (Diisopropylamino)phosphine Dichloride. PCl_3 (4.22 g, 30.8 mmol) and 50 mL of diethyl ether in a 100-mL flask equipped with a paddle stirrer was cooled to −78 °C. Diisopropylamine (5.5 g, 55 mmol) was added dropwise with vigorous stirring. The white suspension was allowed to warm to room temperature and stirred an additional 1 h. After filtration, volatiles were removed under reduced pressure at room temperature and the resulting oil was distilled under reduced pressure (85–90 °C, 10 Torr) to yield the product as a colorless oil (3.9 g, 70%). ^1H NMR: 3.95 ppm (heptet, area 1) and 1.3 ppm (doublet, area 6). ^{31}P NMR: 168 ppm (singlet).

$[^iPr_2NPO]_3$, Tris[(diisopropylamino)phosphoxane]. An amount (6.4 mL, 8.1 g, 40 mmol) of $(^iPr_2N)PCl_2$ and 11.2 mL (8.1 g, 80 mmol) of triethylamine in 60 mL of THF were chilled in an ice bath. From a dropping funnel, 0.60 mL (30 mmol) of distilled water and 2.8 mL (20 mmol) of triethylamine in 30 mL of THF were added dropwise with rigorous stirring over 2 h. After addition was complete, the reaction mixture was allowed to warm to room temperature and stirred an additional 1 h. The white precipitate of amine hydrochloride was filtered off and the THF filtrate treated with excess hexane-washed NaH for 6 h and filtered. The filtrate was evaporated to dryness and extracted

---

(17) Rheingold, A. L.; DiMaio, A.-J. *Organometallics* **1986**, *5*, 393–394.

(18) King, R. B., Ed. *Organometallics Synthesis*; Academic Press: New York, 1965; p 124.

(19) Doyle, J. R.; Slade, P. E.; Jonassen, H. B. *Inorg. Synth.* **1960**, *6*, 218–219.

(20) King, R. B., Ed. *Organometallic Synthesis*; Academic Press: New York, 1965; p 71.

Table IX. Crystal Data for Complexes 1, 5, 8, and 9

	1	5	8	9
formula	$MoP_3O_8N_3C_{23}H_{42}$	$Cr_2P_5N_5O_{12}C_{37}$	$MoP_4O_8N_4C_{28}$	$PdCl_2P_4O_4N_4C_{24}H_{56}$
fw	648.73	965.28	754.27	765.66
space group	$Pbc2_1$	$P2_1/c$	$A2/a$	$C2/c$
	orthorhombic	monoclinic	monoclinic	monoclinic
a, Å	11.570 (2)	12.6554 (8)	18.992 (1)	19.980 (5)
b, Å	18.729 (5)	17.6389 (11)	11.306 (5)	11.0945 (10)
c, Å	32.056 (3)	23.6698 (11)	19.368 (1)	17.934 (9)
β, deg		101.82 (1)	98.63 (1)	112.04 (3)
Z	8	4	4	4
d_{calc}, g cm^{-1}	1.241	1.240	1.219	1.381
μ, mm^{-1}	4.83	0.37	0.51	7.48
cryst dimens, mm	0.15 × 0.30 × 0.35	0.25 × 0.25 × 0.30	0.20 × 0.30 × 0.35	0.30 × 0.20 × 0.20
radiation (λ, Å)	Cu Kα (λ = 1.540 56)	Mo Kα (λ = 0.710 69)	Mo Kα	Cu Kα
data collcd	$0° < 2\theta < 120°$	$0° < 2\theta < 44.8°$	$0° < 2\theta < 44.7°$	$0° < 2\theta < 139.9°$
scan	$\theta/2\theta$	$\theta/2\theta$	$\theta/2\theta$	$\theta/2\theta$
no. of unique reflcns	5272	6667	2630	3500
no. of obsd reflcns	3469	4337	2219	3246
$F(000)$	2815.30	1599.76	1671.61	1599.81
R_F	0.047	0.088	0.062	0.051
R_{wF}	0.048	0.081	0.057	0.060

with 20 mL of hexane and filtered. The extracts were evaporated and checked for purity by ^{31}P NMR spectroscopy before use in subsequent reactions.

$Mo(CO)_4[^iPr_2NPO]_3$ (7). The triphosphoxane $[^iPr_2NPO]_3$ (0.7 g, 1.6 mmol) and 0.48 g (1.6 mmol) of $Mo(CO)_4(NBD)$ were dissolved in 15 mL of hexane to give a yellow solution, which was stirred at 20 °C for 12 h. The resulting very pale yellow suspension was filtered and the solid washed with cold hexane and dried under reduced pressure to give 410 mg (41%) of analytically pure 7. Anal. Calcd for $C_{22}H_{42}MoN_3O_7P_3$: N, 6.47; C, 40.69; H, 6.47. Found: N, 6.47; C, 40.77; H, 6.79.

Conversion of Complex 7 to Complex 2. NMR samples of 7 in $CDCl_3$ indicated formation of 2 and disappearance of 7 over several days. Quanttative conversion occurred rapidly when solutions of 7 were warmed to 80–100 °C for 0.5 h. At room temperature and in the solid state, the conversion was slower, requiring several weeks.

$Mo(CO)_4[^iPr_2NPO]_4$ (8a,b). Triphosphoxane (5.0 g, 11.3 mmol) and 3.00 g (11.4 mmol) of $Mo(CO)_6$ were stirred in 120 mL of THF, and the solution was photolyzed by using a Hanovia 450-W medium-pressure mercury lamp. After 20 h, the dark brown solution was evaporated to give a dark oil. This was washed with 20 mL of acetone to give crude 8 as a white, microcrystalline solid (1.4 g, 20% yield based on triphosphoxane). This was recrystallized from hot hexane to give clear crystals of pure 8. Anal. Calcd for $C_{28}H_{56}MoN_4O_8P_4$: N, 7.03; C, 42.24; H, 7.03. Found: N, 6.82; C, 42.07; H, 7.41.

$PdCl_2[^iPr_2NPO]_4$ (9). Triphosphoxane (1.5 g, 3.4 mmol) and 1.0 g (2.6 mmol) of $PdCl_2{\cdot}2PhCN$ were stirred in 30 mL of hexane at room temperature. After 24 h, the orange suspension turned to a yellow color. After filtration, the light yellow residue was washed with hexane and dried under reduced pressure to give 0.8 g (40% based on Pd) of complex 9. Crystals of X-ray quality were obtained by recrystallization from chloroform/hexane mixtures. Anal. Calcd for $C_{24}Cl_2H_{56}N_4O_4P_4Pd$: N, 7.31; C, 37.61; H, 7.31. Found: N, 7.24; C, 37.94; H, 7.58.

$NiBr_2[^iPr_2NPO]_4$ (10). An amount of 0.7 g (1.6 mmol) of triphosphoxane and 0.37 g (1.2 mmol) of $NiBr_2{\cdot}DME$ were stirred in 20 mL of hexane. The orange-red suspension turned brown after 24 h. After filtration and hexane washing, the residue was dissolved in methylene chloride and filtered through Celite to remove any unreacted $NiBr_2{\cdot}DME$. The filtrate was evaporated to give 0.5 g (60% based on Ni) of complex 10 as an orange-red solid. Anal. Calcd for $Br_2C_{24}H_{56}N_4NiO_4P_4$: N, 6.94; C, 35.93; H, 6.94. Found: N, 6.94; C, 35.68; H, 6.94.

X-ray Structural Determination of Complex 1. A summary of crystal data, data collection, and structure refinement details is presented in Table IX. The intensities of a 0.15 × 0.30 × 0.35 mm crystal grown from the slow evaporation of 1 in hexane were collected on a Picker diffractometer. A total of 5316 reflections were measured of which 3469 constituted the unique set considered significant with at the $3\sigma(I_{net})$ level. Absorption corrections were made with minimum and maximum transmission factors of 0.274 and 0.534, respectively. The structure was solved by using MULTAN,[21] and hydrogens were included at calculated positions and refined. Last least squares were calculated with 160 atoms and 685 parameters. Final $R_F = 0.047$ and $R_{wF} = 0.048$ with a GOF of 1.593. All computations were carried out on the NRC-VAX PDP-8e system of programs adapted for the VAX 11/780 computer.[22] Both enantiomers were found in the asymmetric unit but do not differ within experimental limits in their corresponding bond angles and distances. Only one of these has been presented and discussed. Full atomic coordinates as well as anisotropic thermal parameters and structure factor tables are included in the supplementary material.

X-ray Structural Determination of Complex 5. Crystals of 5 were grown from hexane, and a 0.25 × 0.25 × 0.30 mm sample was mounted on a Nonius CAD-4 diffractometer for data collection. A total of 7866 reflections were measured with 6667 of these unique, and 4337 were considered significant with the $2.5\sigma(I_{net})$ criterion. The structure was solved by using MULTAN, but the hydrogen atoms were not located. Disorder of four of the isopropyl groups (at C(21), C(24), C(31), and C(34)) cannot be resolved by using two-site models, and they were refined isotropically only. The last least squares were performed on 61 atoms with 491 parameters. Final $R_F = 0.088$ and $R_{wF} = 0.081$. Atomic fractional coordinates, thermal parameters, and structure factor tables are included in the supplementary material.

X-ray Structural Determination of Complex 8. A 0.20 × 0.30 × 0.35 mm crystal of 8 was mounted on a Nonius CAD-4 diffractometer, and a total of 7142 reflections were collected. Of these 2630 were unique and 2219 were considered significant by using the $2.5\sigma(I_{net})$ criterion. The structure was solved by using MULTAN, and the final least-squares cycles were calculated by using 29 atoms and varying 204 parameters. Hydrogens were not located. The molecule contains a crystallographic 2-fold axis, and the disorder can be accounted for by a two-site model with occupancies of around 0.7 and 0.3 for the umprimed and primed sites, respectively. All atoms were refined anisotropically except the disordered carbons. Final $R_F = 0.062$ and $R_{wF} = 0.057$. Atomic fractional coordinates, thermal parameters, and structure factor tables are included in the supplementary material.

X-ray Structural Determination of Complex 9. A total of 4920 reflections were collected on a 0.30 × 0.20 × 0.20 mm crystal of 9 mounted on a Picker diffractometer. Of these 3500 were unique and 3249 were considered significant by using the $2.5\sigma(I_{net})$ criterion. All non-hydrogen atoms were located, and hydrogens were included in calculated positions and refined. The last least-squares cycles varied 252 parameters for 48 atoms. Final

---

(21) Germain, G.; Main, P.; Woolfson, M. M. *Acta Crystallogr.* **1971**, *A27*, 368–376.

(22) Grant, D. F.; Gabe, E. J. *J. Appl. Crystallogr.* **1978**, *11*, 114–120. Le Page, Y.; Gabe, E. J.; Calvert, L. D. *J. Appl. Crystallogr.* **1979**, *12*, 25–26. Larson, A. C.; Gabe, E. J. *Computing in Crystallography* Delft University Press: Delft, Holland, 1978; p 81.

R_F = 0.051 and R_{wF} = 0.060. Atomic fractional coordinates, thermal parameters, and structure factor tables are included in the supplementary material.

Acknowledgment. We are grateful to the donors of the Petroleum Research Fund, administered by the American Chemical Society, and the National Science Foundation for an instrument grant toward the purchase of the Bruker AM-360 NMR spectrometer. We also thank Dr. Steven P. VanKouwenberg for useful discussions.

Supplementary Material Available: Tables of atomic coordinates, bond angles and distances, and isotropic as well as anisotropic thermal parameters for **1**, **5**, **8**, and **9** (20 pages); tables of observed and calculated structure factors (106 pages). Ordering information is given on any current masthead page.

Clusters Containing Carbene Ligands. 11. Carbene Ligand Transfer. Reaction of $Os_3(CO)_{11}[C(Et)NMe_2]$ with Terminal Alkynes

Richard D. Adams* and Gong Chen

Department of Chemistry, University of South Carolina, Columbia, South Carolina 29208

Received March 18, 1991

The reaction of $Os_3(CO)_{11}[C(Et)NMe_2]$ (**1**) with Bu^tC_2H in the presence of Me_3NO has yielded the new complex $Os_3(CO)_9[C(Et)NMe_2][\mu_3\text{-}C(H)CBu^t]$ (**3**) in 22% yield and the known complex $Os_3(CO)_{10}[\mu\text{-}H_2CNMeC(Et)](\mu\text{-}H)$ (**2**) in 14% yield. When refluxed in hexane solvent for 1.5 h, compound **3** was converted to the three new complexes $Os_3(CO)_8[C(Et)NMe_2][\mu_3\text{-}CCBu^t](\mu\text{-}H)$ (**4**; 35%), $Os_3(CO)_8[C(Et)N(Me)CH_2][\mu_3\text{-}CHCBu^t](\mu\text{-}H)$ (**5**; 43%), and $Os_3(CO)_9[\mu_3\text{-}Bu^tCC\{C(Et)(NMe_2)\}](\mu\text{-}H)$ (**6a**; 8%). The reaction of **1** with PhC_2H in the presence of Me_3NO yielded $Os_3(CO)_9[\mu_3\text{-}PhC_2C(Et)(NMe_2)](\mu\text{-}H)$ (**6b**; 35%). Compound **5** was converted back to **3** (9%) with the formation of some **4** (7%) by reaction with CO at 68 °C/1 atm. Compound **4** was converted to **6a** (60%) by reaction with CO at 102 °C/1000 psi, but no **6a** could be obtained from **4** under the original reaction conditions. The phenyl derivative **6b** was also obtained in 35% yield from the reaction of **1** with PhC_2H at 97 °C without addition of Me_3NO. Compounds **3**–**5** and **6b** were characterized by single-crystal X-ray diffraction analysis. Compound **3** contains a triply bridging Bu^tC_2H ligand and a terminally coordinated ethyl(dimethylamino)carbene ligand. Compound **4** contains a triply bridging *tert*-butylacetylide ligand, terminally coordinated ethyl(dimethylamino)carbene, and a hydride ligand. Compound **5** contains a triply bridging Bu^tC_2H ligand, a hydride, and an ethyl(dimethylamino)carbene ligand that was metalated on one of the *N*-methyl groups. Compound **6b** contains a triply bridging phenyl(ethyl(dimethyliminio)methyl)alkyne ligand that was formed by the transfer of the carbene ligand to the alkyne ligand. Crystal data: for **3**, space group $P2_1$, a = 8.648 (3) Å, b = 12.039 (5) Å, c = 12.084 (2) Å, β = 97.18 (2)°, Z = 2, 1748 reflections, R = 0.025; for **4**, space group $P2_1/n$, a = 10.755 (2) Å, b = 14.669 (4) Å, c = 15.841 (3) Å, β = 96.64 (2)°, Z = 4, 2074 reflections, R = 0.030; for **5**, space group $P2_1/n$, a = 8.623 (4) Å, b = 23.836 (4) Å, c = 11.925 (3) Å, β = 99.92 (1)°, Z = 4, 2705 reflections, R = 0.031; for **6b**, space group $P2_1/n$, a = 9.027 (3) Å, b = 16.051 (4) Å, c = 17.769 (3) Å, β = 93.17 (1)°, Z = 4, 1804 reflections, R = 0.035.

Introduction

Recently, there has been a flurry of interest in the use of metal complexes containing carbene ligands as reagents in organic syntheses.[1] Since there are relatively few examples of transition-metal cluster complexes containing carbene ligands,[2] most studies of organic syntheses with these ligands have been concentrated on mononuclear metal carbene complexes.

We have recently reported the first example of a simple carbene derivative of $Os_3(CO)_{12}$, $Os_3(CO)_{11}[C(Et)NMe_2]$ (**1**).[3] An important and characteristic feature of the organic chemistry of metal cluster complexes is their ability to produce multicenter transformations of organic ligands.[4] As a part of our continuing investigations of the chemistry of this and related complexes, we have studied the nature of the reactions of **1** with the terminal alkynes Bu^tC_2H and PhC_2H. These results are reported here. A preliminary report of this work has been published.[3]

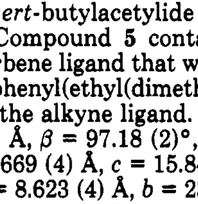

1

Experimental Section

General Methods. All reactions were carried out under an atmosphere of nitrogen. Reagent grade solvents were stored over 4-Å molecular sieves. TLC separations were performed in air on Whatman 0.25-mm silica gel 60-Å F_{254} plates. IR spectra were recorded on a Nicolet 5DXB FT-IR spectrophotometer. ^1H NMR spectra were taken at 300 MHz on a Bruker AM-300 spectrometer. Phenylacetylene and *tert*-butylacetylene were purchased from Aldrich and were used without further purification. $Os_3(CO)_{11}[C(Et)NMe_2]$ (**1**)[3] and $Os_3(CO)_{10}[\mu\text{-}CH_2N(Me)C(Et)](\mu\text{-}H)$ (**2**)[5] were prepared by the previously reported procedures.

---

(1) (a) Collman, J. P.; Hegedus, L. S.; Norton, J. R.; Finke, R. G. *Principles and Applications of Organotransition Metal Chemistry*; University Science Books: Mill Valley, CA, 1987; Chapter 16. (b) Dötz, K. H. In *Transition Metal Carbene Complexes*; Dötz, K. H., Fischer, H., Hofmann, P., Kreissel, F. R., Schubert, U., Weiss, K., Eds.; Verlag Chemie: Weinheim, Germany, 1983.

(2) Adams, R. D. *Chem. Rev.* **1989**, *89*, 1703.

(3) Adams, R. D.; Chen, G. *Organometallics* **1990**, *9*, 2882.

(4) (a) Adams, R. D. In *Metal-Metal Bonds and Clusters in Chemistry and Catalysis*; Fackler, J. P., Jr., Ed.; Plenum: New York, 1990; pp 75–89. (b) Chisholm, M. H. *Ibid.* pp 55–74. (c) Adams, R. D.; Horvath, I. T. *Prog. Inorg. Chem.* **1985**, *33*, 127.

0276-7333/91/2310-3020$02.50/0